Nuclear Materials and Energy 000 (2016) 1–6

Contents lists available at ScienceDirect

Nuclear Materials and Energy

journal homepage: www.elsevier.com/locate/nme

Microstructure and mechanical property in heat affected zone (HAZ) in F82H jointed with SUS316L by fiber laser welding

S. Kano[a,*], A. Oba[b], H.L. Yang[a], Y. Matsukawa[a], Y. Satoh[a], H. Serizawa[c], H. Sakasegawa[d], H. Tanigawa[d], H. Abe[a,e]

[a] Institute for Materials Research, Tohoku University, 2-1-1 Katahira, Aoba-ku, Sendai, Miyagi 980-8577, Japan
[b] Graduate School of Engineering, Tohoku University, 6-6-01-2 Aobayama, Sendai 980-8579, Japan
[c] Joining and Welding Research Institute, Osaka University, 11-1 Mihogaoka, Ibaraki, Osaka 567-0047, Japan
[d] Japan Atomic Energy Egency (JAEA), Fusion Research and Development Directorate, Division of Rokassho BA Project, Structural Materials Development Group, 2-166 Omotedate, Obuchi, Rokkasho, Aomori 039-3212, Japan
[e] Department of Nuclear Engineering, School of Engineering, The University of Tokyo, 2-22 Shirakata Shirane, Tokai, Ibaraki 319-1188, Japan

ARTICLE INFO

Article history:
Available online xxx

Keywords:
Fiber laser welding
Dissimilar joint
F82H
$M_{23}C_6$
HAZ
Nano-indentation hardness

ABSTRACT

This study investigates the microstructure and mechanical property in heat affected zone (HAZ) between F82H and SUS316L jointed by 4 kW fiber laser welding at different parameters such as laser scan rate and beam position. OM/FE-SEM observation, EPMA analysis and nano-indentation hardness test were utilized to characterize the microstructure and evaluate the mechanical property. Results show that the HAZ width is dependent on the welding condition. The precipitation of $M_{23}C_6$ particle in HAZ is found to be closely related to the distance from WM/HAZ interface. Decrease in Cr and C concentration in $M_{23}C_6$ depended on the welding condition; the decrease was relatively milder in the case of shifting the beam position to SUS side. Furthermore, the rapid increment in nano-indentation hardness, i.e. ≈2500 MPa, at HAZ/F82H interface was observed regardless of welding parameters. The temperatures at HAZ/F82H interface were estimated from Cr and C concentration change of $M_{23}C_6$ by EPMA. It was revealed that the temperature of HAZ/F82H interface increased with increasing HAZ width, and that the presence of over-tempered HAZ (THAZ) region is confirmed only in the specimens welded right on the F82H/SUS interface (no-shift) at the laser scan rate of 3 m/min.

1. Introduction

F82H steels are regarded as one of the candidate structure materials for fusion blanket system. Weldability of them is highly essential to their practical applications, because welding is an inevitable process for box-shaped breeding blanket system [1]. For instance, the water-cooling pipe made by F82H in the blanket system has to be jointed with the cooling pipe made by SUS316L steel in ITER, which makes the dissimilar joining technique between F82H and SUS316L steel indispensable. To date, many investigations on welded F82H have been reported. Techniques such as tungsten inert gas (TIG) welding [2], friction stir welding (FSW) [3], electron beam (EB) welding [4] and fiber laser welding [5] have been employed to weld F82H. Fiber laser welding is a relatively newly-developed technique and currently regarded as one of the most promising methods, due to its high speed and deep penetration, as well as high efficiency, high power and high beam quality [6]. Serizawa et.al., [5] pointed out the advances of the fiber laser welding such as its availability in low vacuum environment and relatively low distortion and residual stress caused by welding than other techniques, and concluded that the fiber laser welding is a suitable way to joint F82H and SUS316L materials.

The practical performance of welded F82H such as creep and irradiation integrity is significantly influenced by the microstructure of heat affected zone (HAZ) in F82H [7], particularly the precipitates: $M_{23}C_6$ (M = Cr, W and Fe) and MX (M = Ta, V; X = C, N) [8,9]. However, these precipitates would undergo distinct change caused by the very high heat input during the welding. The microstructural change is presumed to influence mechanical properties. Undoubtedly, the microstructure of HAZ is directly influenced by the welding parameters such as beam energy, laser scan rate and beam position [10], all of which would affect the maximum temperature, its duration and cooling rate. Nevertheless, the effects

* Corresponding author.
E-mail address: kano.sho0215@gmail.com (S. Kano).

http://dx.doi.org/10.1016/j.nme.2016.08.004

Table 1
Chemical compositions of F82H and SUS316L (wt.%).

	C	Si	Mn	Ni	Cr	Mo	W	Ta	V	Fe
F82H	0.097	0.1	0.44	< 0.002	7.81	< 0.002	1.84	0.058	0.2	Bal.
SUS316L	0.021	0.73	0.99	12.13	17.25	2.11	-	-	-	Bal.

Table 2
Fiber laser welding parameters.

Sample name	Power (kW)	Beam spot (mm)	Thickness (mm)	Shift (mm)	Scan Speed (m/min)
3 m/min No shift	4	0.2	4	0	3
4 m/min No shift				0	4
4 m/min 0.2mm shift				0.2	4

of welding parameters in fiber laser welding still has not yet been well-understood, especially in the dissimilar joint between F82H and SUS316L.

On the other hand, special attention is better to be paid to the precipitation behavior in the HAZ region formed in laser fiber welded F82H. It is reported that the precipitation behavior of $M_{23}C_6$ in HAZ and weld metal (WM) regions of F82H welded by TIG was different from base metal of F82H, when being subjected to thermal ageing and irradiation [11], which may also happen in the HAZ redoing of laser fiber welded F82H. The stability of the fine particles in F82H especially in HAZ region is significantly important for the mechanical performance when comes to the practical application of piping in blanket system. The mechanism of the common failure in the piping due to creep deformation, also named type-4 cracking, is believed to be related to the decomposition of the fine particles [12]. Therefore, it is necessary to clarify the precipitation behavior of fine particles in HAZ region formed in laser fiber welded F82H.

Therefore, the purpose of the present study is to evaluate of the microstructure in HAZ formed by fiber laser welding between F82H and SUS316L (SUS) steel at different welding parameters, such as laser scan rate and laser beam position in order to probe the effect of welding parameters on the formation of microstructure. In particularly, the microstructural analyses were carried out by mainly focusing on the precipitation of $M_{23}C_6$ particles in the region of HAZ formed in F82H steel.

2. Experimental procedure

F82H and SUS plates whose sizes were 100 mm in length, 50 mm in width and 4 mm in thickness were used as experimental materials. The chemical compositions of these materials are shown in Table 1. Before welding, F82H was normalized at 1313 K for 1.8 ks and tempered at 1023 K for 5.4 ks. Welding conditions are summarized in Table 2. Taking the fixed laser power (4 kW), two kinds of laser beam position were applied; one is right on the contact face, and the other one is 0.2 mm shifting to SUS side. Object of this technique is to minimize the microstructure change of F82H from as-heat treated specimen due to the welding heat input. Also, the laser scan rate which is identical to the welding speed was taken as one of experimental parameters, namely 3 and 4 m/min in this work. Hereafter, the samples will be named after the welding parameter. For example, “3 m/min No shift” stands for the specimen welded at the laser scan rate of 3 m/min and the beam position right on the contact face, and “4 m/min 0.2 mm shift” stands for the specimen welded at the laser scan rate of 4 m/min and the beam position of 0.2 mm in SUS side from the F82H/SUS contact face.

Microstructure characterization was performed by an optical microscope (OM), a field-emission scanning electron microscope (FE-SEM) and a field-emission electron probe micro analyzer (EPMA). Electron accelerating voltage and scanning step of EPMA were 30 kV and 0.06 μm, respectively. The average concentration and standard deviation of Cr and C were derived from 30 particles in the EPMA mapping image. Nano-indentation hardness test (SHIMADZU Co., DUH-211s) was performed, the evaluation of mechanical property associated with the distance from the F82H/SUS contact face was carried out to identify the character of microstructure of local area of HAZ. Indentation depth was set as 0.25 μm and the nano-hardness (H_{it}) was calculated by Olver-Pharr method [13]. The area subjected to nano-indentation tests were 600 μm in length and 100 μm in width in order to cover sufficient regions in SUS, weld metal, HAZ and F82H. The distance between the neighbor indentations in hardness test was 10 μm.

3. Results

3.1. Decomposition of $M_{23}C_6$ particle in HAZ

The optical micrographs (OM) and Secondary electron micrographs (SE) of 3 m/min No shif, 4 m/min No shift and 4 m/min 0.2 mm shift specimens are shown in Fig. 1. In all of welding condition specimens, from either SE or OM micrographs, it is clearly seen that the as-welded specimens could be divided into four distinct parts: base metal of F82H, HAZ in F82H (HAZ), weld metal (WM), and base metal of SUS. WM/HAZ and HAZ/F82H interfaces are noted by dot lines, respectively. The average HAZ width of 3 m/min No shift, 4 m/min No shift and 4 m/min 0.2 mm shift specimen was measured as approximately 165, 200 and 220 μm, respectively.

The dark area in SE micrographs in Fig. 1 indicated the EMPA analyzed regions, which starts from F82H and ends at WM regions. The elemental mapping of Cr and C arranged from F82H to WM are shown in Fig. 2. High contract dot features, some of which agglomerated into line features, were clearly observed in F82H side in the both specimens, indicating the segregation of Cr and C in F82H. The contrast features are presumably $M_{23}C_6$ particles in the original F82H according to our previous study [14,15]. The distribution of the particles was attributed from the preferential precipitation of $M_{23}C_6$ particles along grain boundaries, such as prior austenite, packet, block and lath. Note that the Cr segregation was substantially obvious in F82H side, besides, the Cr intensity gradually decreased when the position shifted to WM side. On the other hand, it is also noteworthy that the C segregation was preferentially detected in the F82H and the adjacent HAZ regions. With respect to the observations, it is presumed that $M_{23}C_6$ was present in the area nearby HAZ/F82H interface and it gradually disappeared at the midway HAZ, and that precipitate was absent in the periphery of WM/HAZ interface. And such phenomena were noted in all

Please cite this article as: S. Kano et al., Microstructure and mechanical property in heat affected zone (HAZ) in F82H jointed with SUS316L by fiber laser welding, Nuclear Materials and Energy (2016), http://dx.doi.org/10.1016/j.nme.2016.08.004

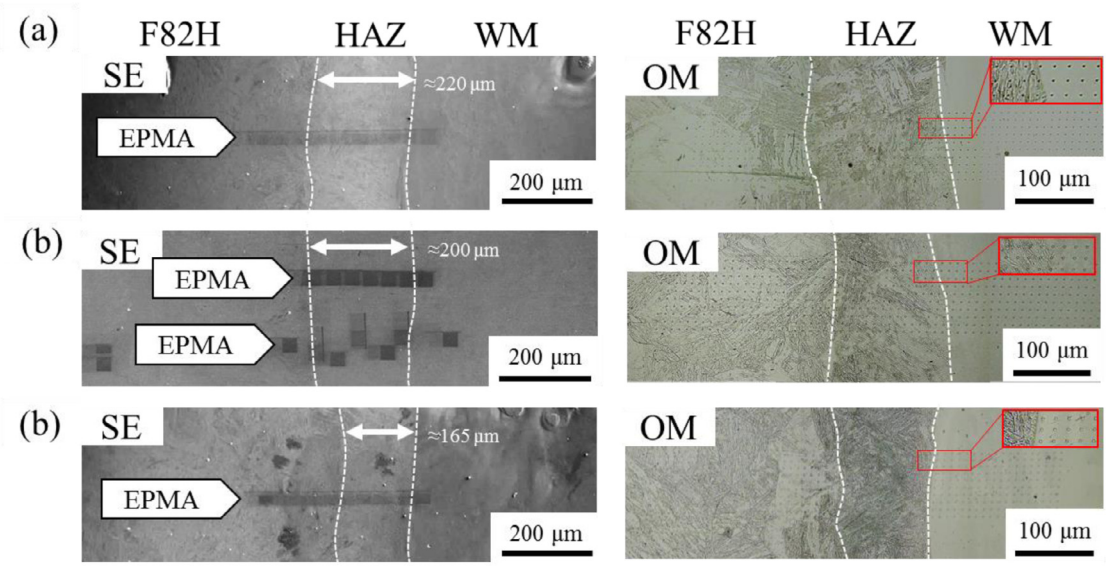

Figure 1. Secondary electron image (SE) and optical microphotograph (OM) of dissimilar joint material under fiber laser welding after EPMA analyses and nano-indentation hardness test of (a) 3 m/min No shift, (b) 4 m/min No shift and (c) 4 m/min 0.2mm shift specimens. Low-contrast spots in SEI are contamination by EPMA analysis. WM/HAZ and HAZ/F82H interface indicate chain line. Average HAZ width of (a), (b) and (c) were 220, 200 and 165 μm, respectively.

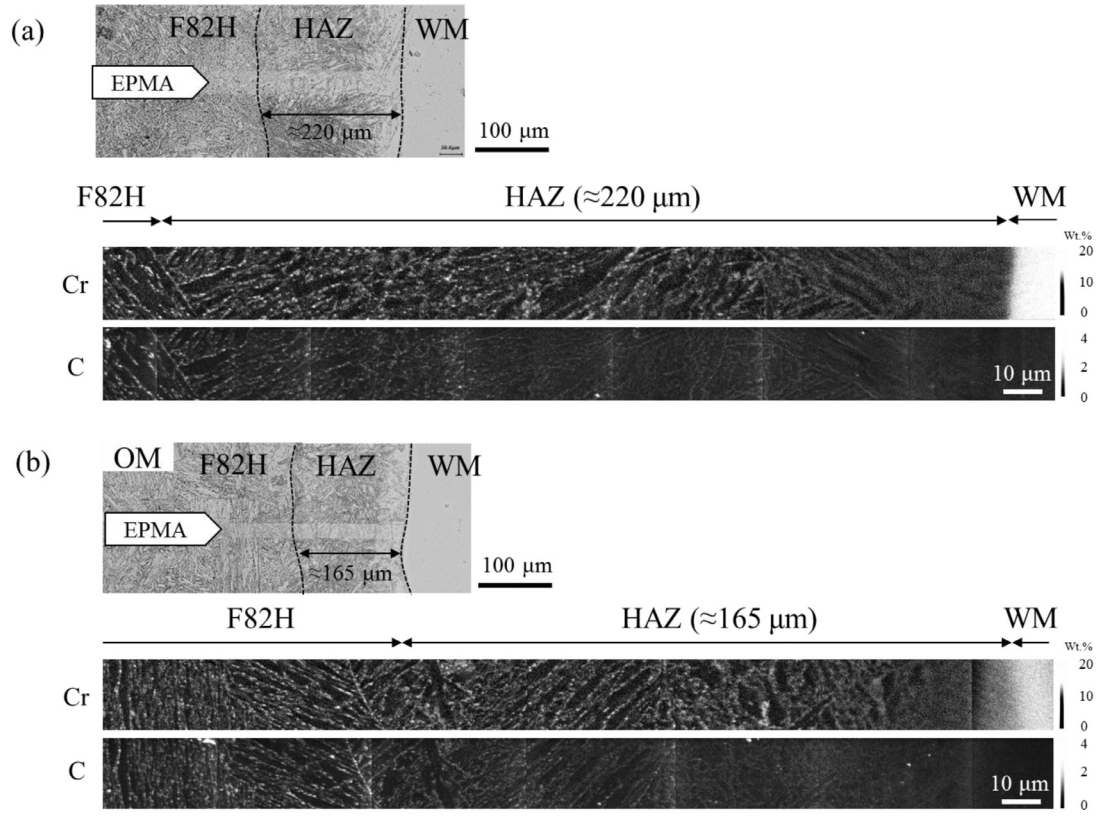

Figure 2. OM and Cr and C mapping images in HAZ of (a) 3 m/min No shift and (b) 4 m/min 0.2mm shift specimens.

the specimens, regardless of beam speed and beam position. To our knowledge, the phenomena were firstly reported.

The Cr and C concentrations in $M_{23}C_6$ achieved from EPMA mapping taken at different region are plotted with the distance from WM/HAZ interface, which is shown in Fig. 3. HAZ and F82H regions were indicated by arrows, respectively. The average Cr and C concentrations in $M_{23}C_6$ were respectively analyzed as 14.8 and 0.72 wt.% in both specimens. Comparing to the chemical composition of $M_{23}C_6$ in F82H matrix measured by TEM/EDS, i.e. 61 and 13 wt.% for Cr and C, respectively [7,11], fairly low level of Cr and C concentration was detected in HAZ. This difference is presumably caused by the instrumental error. Characteristic X-rays detected in EPMA contain signals from a certain volume which is much larger than the probe size due to the scattering the electron beam inside specimen [16]. Although the probe size and the sampling step of EPMA analyses employed in present study were about 100 nm and 60 nm, the estimated diameter of the volume which attributes to the characteristic X-ray was roughly 400 nm. Since the

Please cite this article as: S. Kano et al., Microstructure and mechanical property in heat affected zone (HAZ) in F82H jointed with SUS316L by fiber laser welding, Nuclear Materials and Energy (2016), http://dx.doi.org/10.1016/j.nme.2016.08.004

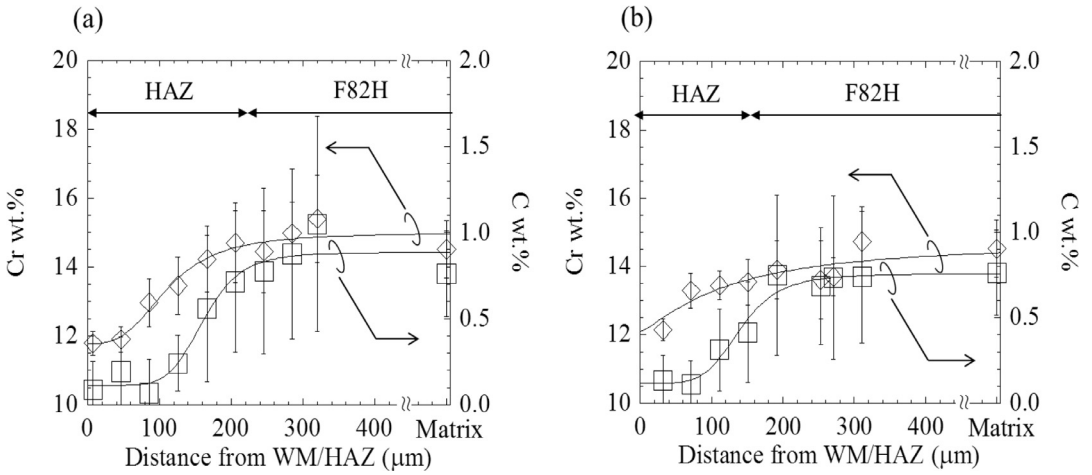

Figure 3. Cr and C concentrations of precipitates in (a) 3 m/min No shift and (b) 4 m/min 0.2mm shift specimens as a function of the distance from WM/HAZ interface. Error bars indicate the standard deviation of measurement from 30 precipitates for each location.

average size of $M_{23}C_6$ in F82H was approximately 100 nm [7,11], the measured composition here contains the signals both from precipitates and matrix, the latter of which contains the lower concentration of Cr and C than the former. Besides the concentrations are in fact less quantitative, their relative variation is still meaningful, from which it is able to investigate the precipitation behavior of these alloying atoms. Furthermore, EPMA allows us to measure tens or hundreds of precipitates at once, which enhances statistical accuracy.

Overall, it is noted that, in both of the specimens, both of Cr and C concentrations in precipitates were relatively higher at the F82H side, they subsequently decreased from the F82H/HAZ interface until roughly stabilized in the HAZ/WM interface. Thus, it is clear that the segregation of Cr and C in HAZ is closely related to the distance from WM/HAZ interface, presumably introduced by the sharp heat gradient from welding side to F82H matrix side. Meanwhile, the Cr and C concentrations in "3 m/min No shift" specimen were different from those in "4 m/min 0.2 mm shift" specimen at both the F82H matrix side and HAZ/WM interface. Furthermore, the decreasing trend in "3 m/min No shift" specimen was relatively gentler, as compared with the welding condition of "4 m/min No shift specimen" [12]. Therefore, it is concluded that precipitation of $M_{23}C_6$ was influenced not only by the location but also the welding parameter such as scan rate and welding position.

3.2. Nano-indentation hardness

Fig. 4 shows the variation of nano-indentation hardness with the distance from WM/HAZ interface under several fiber laser welding conditions. The F82H/HAZ and HAZ/WM interfaces indicated as dot lines and HAZ/WM interface was set to zero. Average of H_{it} in F82H, HAZ and WM were estimated roughly as 3014, 5443 and 5224 MPa, respectively. This revealed that the mechanical properties of as-welded specimen were unchanged by the scan rate and welding position, although the microstructure was affected, for instance: the higher scan rate seems result in a relatively narrower HAZ region (see Fig. 1). Moreover, the rapid increase of H_{it} was detected at HAZ/F82H interface in all the specimens. The abrupt hardness increment from F82H to HAZ was approximately 2500 MPa. It is considered that the H_{it} increment happened at the HAZ/F82H interface is presumably attributable to the martensitic transformation due to the drastic heat input and rapid cooling by laser beam welding. This suggested that the maximum temperature in HAZ region was above Ac_1.

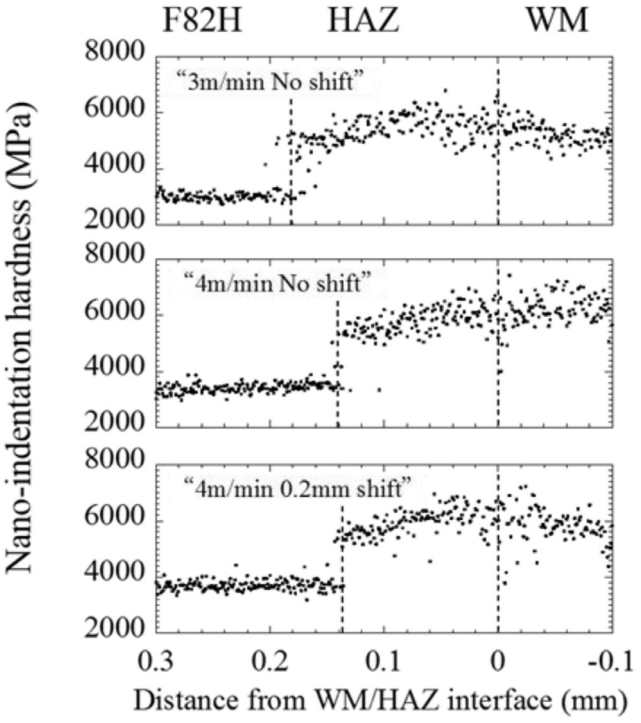

Figure 4. Variation of nano-indentation hardness with the distance from WM/HAZ interface under several fiber laser welding conditions.

4. Discussions

4.1. Assessment of temperature gradient in HAZ

The temperature gradient in HAZ has been assessed from Cr and C concentration change in precipitates evaluated by EPMA in our previous study [14], this technique is that the equivalent thermal equilibrium temperatures in various regions in HAZ could be calculated based on the data set in annealed specimens; the mathematical relationship between the temperature and Cr and C concentration of $M_{23}C_6$ particle express the four dimensions logistic curve fitting formula, the temperature in HAZ calculated from correlation between chemical composition change of precipitate at each region in HAZ and annealing temperature. Similarly, temperature gradients of HAZ in all the specimens measured

Please cite this article as: S. Kano et al., Microstructure and mechanical property in heat affected zone (HAZ) in F82H jointed with SUS316L by fiber laser welding, Nuclear Materials and Energy (2016), http://dx.doi.org/10.1016/j.nme.2016.08.004

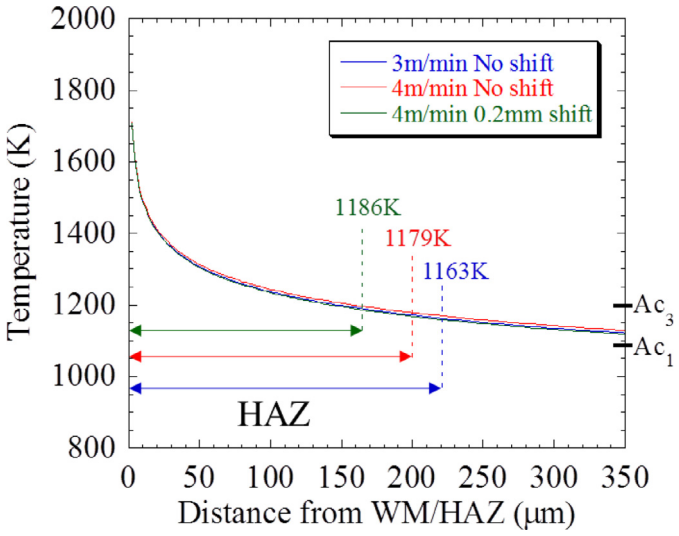

Figure 5. Dependence of temperature on distance from WM/HAZ interface under several fiber laser welding conditions calculated by Cr/C concentration in M23C6 precipitate. Ac1 and Ac3 temperatures of F82H steel are 1089 and 1198 K, respectively.

from the decomposition of $M_{23}C_6$ are shown in Fig. 5. These temperature gradients were estimated from the average value of Cr and C concentration in precipitates and assumed that the temperature in WM/HAZ interface be the melting point of Fe-8Cr-2W-0.1C steel calculated by Thermo-Calc software, i.e.: 1890 K. As noted from Fig. 5, the temperature gradients of all the specimens show high similarity; the temperature suddenly decreased with the decreasing distance from the WM/HAZ interface, this decreasing rate in range from less than 5 μm near WM/HAZ interface was approximately 60 K/μm. Furthermore, the highest temperature experienced at HAZ/F82H interface was estimated as 1163, 1179 and 1186 K for 3 m/min No shift, 4 m/min No shift and 4 m/min 0.2 mm shift specimens, respectively. These temperatures are roughly equivalent to the middle temperature range between Ac_1 and Ac_3 [17]. However, this estimation is unable to explain the γ phase formation because the $\alpha \rightarrow \gamma$ transformation temperature may be higher under the non-equilibrium annealing condition in such laser welding process. In other words, the heat that is necessary to rearrange of crystal structure is overestimated from the static thermal equilibrium condition. Therefore, the accurate determination of the temperature in HAZ during welding may not be provided only by the chemical composition variation in $M_{23}C_6$, even though the detail of phase transformation during fiber laser welding is unclear. But, from the temperatures at HAZ/F82H interface estimated from Fig. 5, it is found the temperature at HAZ/F82H interface decreased with increasing HAZ width, which is fairly reasonable because the wider HAZ width leads to a further distance away from the welding point.

4.2. Over-tempered HAZ (THAZ)

As revealed from the C and Cr chemical composition change of $M_{23}C_6$ in HAZ (see Fig. 3), it is found that the Cr and C concentrations at the location of 330 μm away from the WM/HAZ interface in 3 m/min No shift specimen was higher than the matrix of F82H. According to our previous study [14], in which the F82H was equilibrium thermally annealed at various temperatures ranging from 1073 to 1323 K and followed by air cooling, the Cr and C concentrations of precipitate in 1073 K annealed specimen were respectively 16.7 and 1.3 wt.%, these values are slightly higher than those in the original F82H, i.e. 14.8 wt.%Cr and 0.72 wt.%C. Thus, it was concluded that the average C and Cr concentration of precipitate increased compared to the matrix due to the annealing at higher than the tempering temperature condition. Beside, as indicated previously, the HAZ formed by fiber laser welding between F82H and SUS316L is identified to contain two regions: coarse grain HAZ (CGHAZ) and fine grain HAZ (FGHAZ). But, the over-tempered HAZ (THAZ) region was not observed. Tanigawa et.al., [2] reported that the THAZ region existed beyond the FGHAZ region in TIG-welded F82H. The microstructural features in THAZ were grain coarsening and recovery due to the annealing effect by strong welding heat input, which resulted in the decreasing of strength. This is because the maximum temperature in this region experienced during welding is estimated 1023 K, which is lower than Ac_1. Nevertheless, the chemical composition of $M_{23}C_6$ in THAZ has not been studied yet. In present study it is clearly demonstrated that the Cr and C concentration in $M_{23}C_6$ was higher in the specimen annealed above tempering temperature, presumably controlled by the Ostwald ripening [18]. Furthermore, as revealed from EBSD analysis, the significant grain size change of martensite was not observed at the location periphery 330 μm away from WM/HAZ interface in 3 m/min No shift specimen, despite that the grain growth was supposed to occur at the THAZ region based on the theoretical thermal distribution under welding. The absence of grain growth in this region is probably because that the welding heat input by fiber laser is extremely high and the heating and cooling rate is extremely fast, leaving scarcely any time needed for grain growth. Therefore, based on the microstructure analysis it is considered that the THAZ region locates 330 μm away from WM/HAZ interface in 3 m/min No shift specimen. However, the decrease of H_{it} was not observed in the region, this is because the microstructure change caused by rapidly heating and cooling during fiber laser welding was not obvious.

5. Conclusions

To investigate the effects of fiber laser welding parameters on microstructure and mechanical property, SEM/OM observation, EPMA analysis and nano-indentation hardness test were performed on specimens prepared at different welding speeds and beam positions. It is observed that HAZ width was influenced by welding speed and beam position; the HAZ width of 3 m/min No shift and 4 m/min 0.2 mm shift specimens were 220 and 165 μm, respectively. However, those welding parameters affected trivial on the nano-indentation hardness of WM and HAZ. Besides, the decomposition of $M_{23}C_6$ in HAZ was found to be closely correlated to the distance from WM/HAZ interface, regardless of the welding speed and beam position. Decrease in Cr and C concentration in $M_{23}C_6$ was observed and was relatively mild in the specimens exposed to the shifting of the beam position to SUS. Furthermore, the temperature at HAZ/F82H interface under different welding parameter was estimated from Cr and C concentration variation in $M_{23}C_6$. Based on the composition measurement of $M_{23}C_6$, temperature at the HAZ/F82H interface is higher in wide HAZ specimen, while the THAZ was analyzed to be present in the specimen welded at slower rate.

Acknowledgments

A part of this work was supported by the Japanese Implementing Agency under the Procurement Number IFERC-T3PA03-JA within the “Broader Approach Agreement” between the Government of Japan and the European Atomic Energy Community. This Work was performed under the Joint Usage/Research Center on Joining and Welding, Osaka University.

References

[1] T. Hirose, H. Sakasegawa, M. Nakjima, H. Tanigawa, Fusion Eng. Design (2015) (In press).
[2] H. Tanigawa, M. Ando, T. Sawai, K. Shiba, N. Hashimoto, R.L. Klueh, Fusion Sci. Tech. 44 (2003) 219–223.
[3] D.T. Hoelzer, K.A. Unocic, M.A. Sokolov, Z. Feng, J. Nucl. Mater. 442 (2013) S529–S534.
[4] N. Hara, S. Nogami, T. Nagasaka, A. Hasegawa, H. Tanigawa, T. Muroga, Fusion Sci. Tech. 56 (2009) 318–322.
[5] H. Serizawa, D. Mori, Y. Shirai, H. Ogiwara, H. Mori, Fusion Eng. Design 88 (2013) 2466–2470.
[6] Y. Kawahito, M. Mizutani, S. Katayama, J. Appl. Phys. D 40 (2007) 5854–5859.
[7] X. Jia, T. Dai, J. Nucl. Mater. 343 (2005) 212–218.
[8] F. Abe, S. Nakazawa, H. Araki, T. Noda, Metal. Mater. TransA 23 (1992) 469–477.
[9] K. Sawada, K. Kubo, F. Abe, J. Mater. Sci. Tech. 19 (2003) 732–738.
[10] B.L. Shultz, C.E. Jackson, Welding J. 52 (1973) S26–S37.
[11] X. Jia, T. Dai, J. Nucl. Mater. 329-333 (2004) 309–313.
[12] K. Sawada, M. Tabuchi, H. Hongo, K. Kimura, Mater. Characterixation 59 (2008) 1161–1167.
[13] W.C. Olver, G.M. Pharr, J. Mater. Res. 19 (2004) 4–20.
[14] K. Sho, A. Oba, H.L. Yang, Y. Matsukawa, Y. Satoh, H. Serizawa, H. Sakasegawa, H. Tanigawa, H. Abe, Mech. Eng. Lett. 15 (2015) 00481.
[15] H. Sakasegawa, H. Tanigawa, S. Kano, M. Enomoto, Fusion Eng. Design 86 (2011) 2541–2544.
[16] K. Kanaya, S. Okayama, J. Appl. Phys. 5 (1972) 43–59.
[17] T. Sawai, E. Wakai, T. Tomita, A. Naito, S. Jitsukawa, J. Nucl. Mater. 307-311 (2002) 312–316.
[18] F. Abe, Sci. Technol. Adv. Mater. 9 (2008) 013002(15pp).

Please cite this article as: S. Kano et al., Microstructure and mechanical property in heat affected zone (HAZ) in F82H jointed with SUS316L by fiber laser welding, Nuclear Materials and Energy (2016), http://dx.doi.org/10.1016/j.nme.2016.08.004